# SOME FEATURES OF THE TURBULENCE PRODUCED BY RISING AIR BUBBLES IN WATER\*

JIA Fu (贾 复), LIU YI-NIAN (柳绮年) AND CHEN XUE-WU (陈学武)
(Institute of Mechanics, Academia Sinica, Beijing 100080, PRC)

Received April 4, 1990.

#### ABSTRACT

Presented in this paper is an experimental study on the characteristics of the turbulence produced by rising air bubbles in water. The measurements of turbulent velocities were made by using visualization technique of particle streak and computer image processing of the flow field. The turbulence features have been examined, showing that the rising bubble-produced turbulence can be approximately modeled by homogeneous turbulence as in the case of grid turbulence in air.

Keywords: turbulence, bubbles, image processing.

#### I. Introduction

The rising movement of gas bubbles in liquid phase media is a common phenomenon either in nature or in some technological processes in chemical and heat transfer engineerings. The motions of rising bubbles have significant effects on heat and mass transfer processes between bubbles and ambient liquid. So far investigations have been mainly performed on the kinetic and dynamic behaviors of single bubble or group of bubbles rather than on the motion of ambient liquid media produced. The study of the latter is more difficult, but at the same time, more significant in view of some engineering applications, for example, the problem of mass transfer between gas bubbles and ambient fluid would be much simplified if the state of turbulent motion of the latter is clear<sup>[1]</sup>.

As a preliminary step of general study on the turbulent motion of fluid produced by rising bubbles, we experimentally examined the water motion agitated by rising bubbles, which were released simultaneously and spatially uniformly from a horizontal plane. Additional interest for looking at the features of turbulence so produced lies in the possibility of using the rising bubbles as a turbulence generator in liquid as in the case for grid turbulence in air. Since the classic investigation of grid turbulence by Batchelor and Townsend<sup>[2]</sup>, the grid turbulence has been extensively used as a useful configuration for looking at more complicated turbulent motions, as exemplified by the recent works of Turner<sup>[3]</sup> and Britter et al.<sup>[4]</sup> In the

<sup>\*</sup> Project supported by the National Natural Science Foundation of China.

experimental studies of turbulent mixing across density interface, the bubble turbulence may create a situation of combined internal and external mixing<sup>15]</sup>. It is expected that such a turbulence system may be beneficial for some turbulence studies.

## II. EQUIPMENT, INSTRUMENTATION AND DATA ANALYSIS

The experiments were conducted in a perspex tank,  $25 \times 25$  cm<sup>2</sup> in bottom area and 60 cm in height, as shown in Fig. 1. An air bubble generator—a chamber with a replaceable upper lid was located at the bottom of the tank. The upper lids were perforated uniformly. The diameter of small holes was 0.6 mm. Three upper lids with different distances between holes, denoted by  $M_b$ ,  $M_b = 2.5$ , 4, 6 cm were used. The air in chamber was supplied by a mini-compressor through a decompress valve and an electromagnetic valve. The latter was used to facilitate easy and fast operation of the air bubble releasing. Multi-layer of bubbles was produced by successive operations of the electromagnetic valve at given time intervals. The air pressure in the chamber was 0.02-0.04 Mpa.

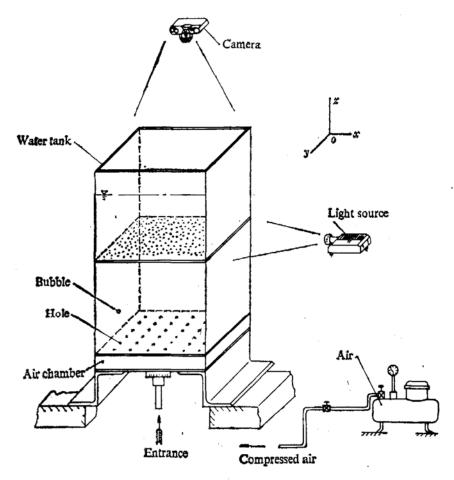


Fig. 1. Schematic diagram of experimental system for bubble turbulence.

The motions of rising bubbles were recorded by a video-recording system. The size, shape, wobbling and rising velocity of bubbles, etc. were measured by replaying the video tape records. Based on the observational data [6], it is suggested that the configurations and motion features of rising bubbles, etc. are characterized by the bubble Reynolds number Re, Eötvös number Eo and material parameter M.

These three parameters stand for the ratios of inertial force to viscous force, buoyance to surface tension and material properties, respectively. They are defined as follows:

$$Re = \frac{\rho d_e U_T}{\mu}, \quad Eo = \frac{g\Delta \rho d_e^2}{\sigma}, \quad M = \frac{g\mu^4\Delta \rho}{\rho^2 \sigma^3},$$
 (1)

where  $d_e$  is the equivalent diameter of the bubbles,  $\rho$ ,  $\Delta \rho$  are the density of liquid and density difference between liquid and air,  $\mu$  is the viscosity of liquid,  $\sigma$ , the surface tension,  $U_T$ , the terminal velocity of bubbles and g, the gravity acceleration. Fig.2(a) and Fig.2(b) show typical rising bubbles of one- and two-layer, respectively. It can be seen in these photographs that the bubbles so produced belong to ellipsoids and wobbling regime<sup>[6]</sup>. The averaged equivalent diameter  $d_e$  was 0.7 cm. The measured terminal velocities of rising bubbles were found to be basically independent of the numbers of bubble layers and  $M_b$ . The terminal velocity  $U_T$  obtained by least squares fitting to experimental results was 22.1 cm/s, as shown in Fig. 3. The experimental conditions calculated according to (1) were

$$Re = 1848, E_0 = 9.04 \sim 10.33, M = 2.485 \times 10^{-11}$$
 (2)

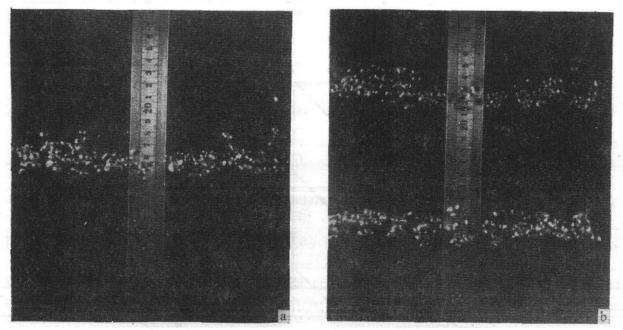


Fig. 2.(a) The rising air bubbles of single layer in water.

(b) The rising air bubbles of 2-layer in water.

The configuration features and the terminal velocity of bubbles observed in the experiments agreed quite satisfactorily with those deducted from the study on single bubble (see Figs. 1.3.23 and 1.3.24 in [6]).

White plastic particles of 0.5 mm diameter were used as tracers of turbulent motion of fluid. The particles were made neutrally buoyant and uniformly distributed in dilute salt water in the tank. A horizontal plane section at the mid-height of the tank was illuminated by a horizontal sheet light. A 135 camera with automatic winder and flash was mounted above the tank pointing downwards to record the particles' streaks during given exposure times. The turbulent motion of fluid

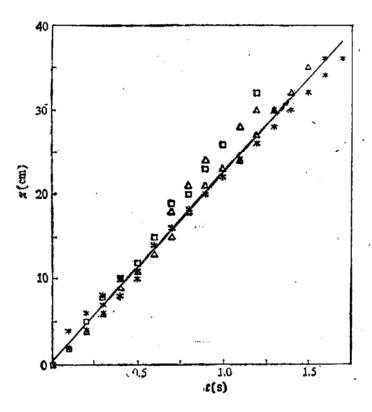


Fig. 3. The averaged displacements of bubbles vs. time t during their rising motions.

was agitated by the rising bubbles of 1,2,3 layers in a fully still water. The evolution processes of the turbulence were recorded in sequential pictures of particle streaks. Shown in Fig. 4 is a typical streak picture representing horizontal velocity field of bubble turbulence. The streaks in the pictures were "read into" a computer manually through a digitizing pad to collect the needed flow field information. The streak data were processed in the following way:

$$\begin{cases}
\widetilde{u}_{i} = \Delta x_{i}/\Delta t, \ \overline{U} = \frac{1}{N} \sum_{i=1}^{N} \widetilde{u}_{i}, \\
u_{i} = \widetilde{u}_{i} - \overline{U}, \ \overline{u}^{2} = \frac{1}{N} \sum_{i=1}^{N} u_{i}^{2},
\end{cases}$$
(3)

where  $\Delta x$  is the x component of *i*th streak (vector),  $\Delta t$ , the exposure time used in experiments, N, the total number of streaks,  $\tilde{u}_i, u_i$  are u component of instantaneous velocity, turbulent velocity of *i*th particle respectively, and  $\bar{U}$  is the component of mean velocity. The corresponding quantities for v component were obtained in the same way. Two point parallel correlations of turbulence velocity were computed in the following way. The distance between a pair of turbulence velocity vectors was computed and the components of the vectors were resolved onto their connecting line. The products of the *i*th pair,  $u_{p_i}$ ,  $u_{p_i'}$ , along with all other pairs within the same photograph were found. All pairs with separation distances lying between  $r - \Delta r/2$  and  $r + \Delta r/2$  were averaged according to

$$\overline{u_{p} \cdot u_{p'}(r)} = \frac{1}{N_{p}} \sum_{i=1}^{N_{p}} u_{p_{i}} \cdot u_{p'_{i}}(r), \qquad (4)$$

where  $N_p$  is the total number of pairs within an interval  $\Delta r$  and r is the mean separation distance.

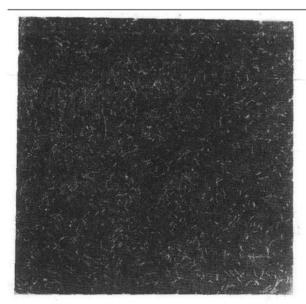


Fig. 4. A photograph of particles' streaks representing the horizontal turbulent velocity field of bubble turbulence.

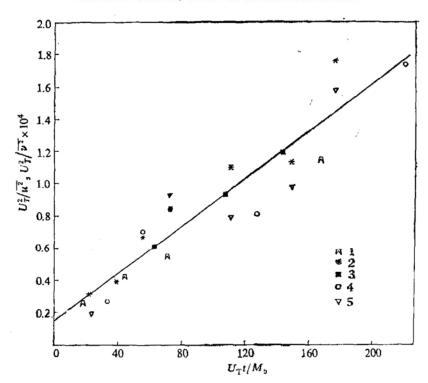


Fig. 5. Decay of turbulent kinetic energy in the course of nondimensional time  $U_{T}t/M_b$  for  $N_e = 1$  with 3  $M_b(\text{cm})$ :  $\triangle$ , 2.5; \*, 4;  $\blacksquare$ , 6; and for  $N_e = 3$ ,  $M_b(\text{cm})$ :  $\bigcirc$ , 4 cm.

The corresponding correlation function is computed as

$$f_{\parallel}(r) = \overline{u_p \cdot u_{p'}/\overline{u_p^2}(r)}. \tag{5}$$

Based on the above-mentioned data-processing procedure and the results, the turbulent kinetic energy, integral scale and Taylor micro-scale can be calculated, as

detailed in Ref. [7].

# III. SOME FEATURES OF RISING BUBBLE-PRODUCED TURBULENCE

Compared with the grid turbulence, which has been intensively investigated and the main results of which were summarized (e.g. Ref. [8]), much less is known about the bubble-produced turbulence. The chief purpose of the present study is then to make clear some primary featuers of the turbulence of this kind, say, the homogeneities of bubble turbulence. With bubble turbulence used as an experimental system of turbulence generator, we are also concerned with the effects of bubbles distance  $M_b$ , the number of bubble layers  $N_e$  on the turbulence intensity, integral scale, etc.

# 1. The Decay Law of Turbulent Kinetic Energy of Bubble Turbulence

The features of grid turbulence decay are formulated by the well-known linear law of  $u^{-2} \propto t$  and  $\lambda^2 \propto t$  ( $\lambda$  is the Taylor microscale of turbulence), which were obtained from grid turbulence experiments in wind tunnels and were assumed to be the universal features of homogeneous turbulence<sup>[9]</sup>. Following the same line of thought we express the present experimental data in a similar form. The measurements of decaying process of turbulent energy for bubble turbulence are shown in Fig. 5 for  $M_b = 2.5$ ,4,6 cm and  $N_e = 3$  (for  $M_b = 4$  cm). It is seen that up to  $U_T t/M_b = 200$  the energe decay basically obeys the "classic linear decay law" of homogeneous turbulence during the initial period of turbulent decay. The least square fitting to the measurements can be expressed as

$$U_{\rm T}/\overline{u^2} = \alpha (U_{\rm T}t/M_{\rm b} - U_{\rm T}t_0/M_{\rm b}), \tag{6}$$

where  $\alpha=72.4$  and  $t_0=-2.4$ s, determined by the present experiments. Also included in Fig. 5 is the energy decay law for component v. We see that, up to  $U_T t/M_b < 100-150$  the ratio of squares of x-and y-turbulent velocities  $u^2/v^2 < 1.1$ , satisfying a proposed criterion for the homogeneity of turbulence.

The turbulence created by multi-layer rising bubbles is obviously more intense than that produced by single layer bubbles. The processed data for the turbulence agitated by 3-layer bubbles indicate that the turbulent energy  $\overline{u^2}$  roughly obeys the same decay law as the single layer bubble turbulence. One third of the measured turbulent kinetic energy of 3-layer bubbles is plotted and included in Fig. 5. The results turn out to collapse the decay law of turbulence for single layer of bubbles. Besides, the intensity of bubble turbulence is much weaker than that of grid turbulence.

## 2. The Self-preservation of Double Correlation Function of Turbulences

The so-called self-preservation of double or the second and triple or third velocity correlation, which was observed and addressed in grid turbulence study<sup>[9]</sup> means that the 2nd and 3rd correlation functions f(r) and k(r) can be approximately expressed as functions of  $r/\lambda$  only during the initial decaying process, independent of time t. Such are the basis for some theoretical deduction of homogeneous turbu-

lence. From turbulent energy equation

$$du^2/dt = -10v\overline{u^2}/\lambda^2 \tag{7}$$

and the initial period of decay law

$$\lambda^2 = 10\nu t, \tag{8}$$

we examined the self-preservation of the 2nd correlation of the bubble turbulence. Though, as shown in Fig. 5, the bubble turbulence decays in a way quite close to the initial period of decay law of homogeneous turbulence up to  $U_{\rm T}t/M_{\rm b}$ —200, the physical lapse time is about 30—40 s, much longer than that of grid turbulence in air. From the theory of homogeneous turbulence we have

$$\overline{u^2}/\lambda^2 = \overline{(\partial u/\partial x)^2}, \qquad (9)$$

which implies that the  $\lambda^2$  can be calculated from (9), if the rate of strain  $(\partial u/\partial x)$  and its mean square are obtainable from measurement. As described in [7],  $\frac{\partial u}{\partial x}$ 

can be estimated from streak pictures by averaging  $\Delta u/\Delta x$  over streak pairs in a sufficiently small neighbourhood of sampling points. Fig. 6 shows the  $\lambda^2$  so obtained against time t. It is seen that there exists a rough linear relationship between  $\lambda$  and t. If we further assume that the relation  $\lambda^2 = k\nu t$  holds for bubble turbulence then the measurement agrees with the above relation quite well provided k = 3. In Fig. 7(a) are shown the plots of the experimental results of  $f_{\parallel}$  as a function of  $r/\lambda$  for 6 different times in decaying process, where the measured values of  $\lambda$  were used. For the sake of comparison, the measured  $f_{\parallel}$  as function of r is shown in Fig. 7(b). From these figures it can be seen that for small value of  $r/\lambda$  ( $r/\lambda < 1$  for instance) the values of  $f_{\parallel}$  at different decaying times are close to each other, the curve of  $f_{\parallel}$  can approximately be regarded as a universal one representing the behavior of self-preservation. This may suggest that the deductions in homogeneous turbulence theory based on self-preservation may also be approximately applied to bubble turbulence.

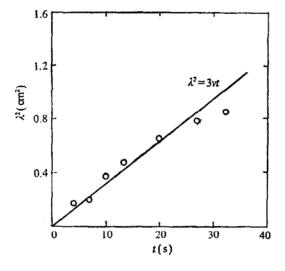


Fig. 6. The relationship between Taylor microscale and time t.

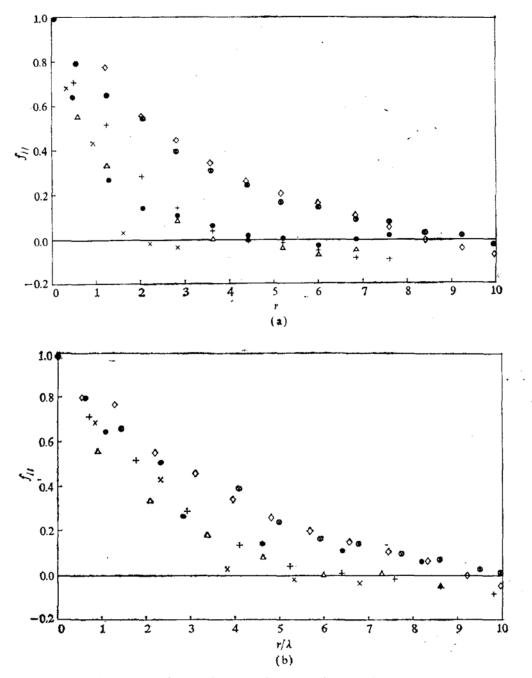


Fig. 7. The 2nd velocity correlation function for bubble turbulence at 6 non-dimensional times  $U_T t/M_b$  ( $N_e=1$ ):  $\times$ , 22.1 ( $\lambda=0.412$ );  $\bullet$ , 38.7 ( $\lambda=0.44$ );  $\triangle$ , 55.3 ( $\lambda=0.606$ ), +, 71.8 ( $\lambda=0.691$ );  $\otimes$ , 149.2 ( $\lambda=0.883$ );  $\diamond$ , 176.8 ( $\lambda=0.916$ ).

(a) Plotted as  $f(r/\lambda,t)$ ; (b) plotted as f(r,t).

The integral scale of turbulence can be computed in term of correlation func-

$$L = \int_0^\infty f_{\parallel}(r)dr. \tag{10}$$

The plots of  $(L/M_b)^2$  vs.  $U_T t/M_b$  for 3 groups of experimental results are shown in Fig. 8. These results show a general trend of linearity between  $U_T t/M_b$  and  $(L/M_b)^2$ , similar to that of grid turbulence. If we assume that such a linear relationship does exist, then once more the homogeneity properties of bubble turbulence

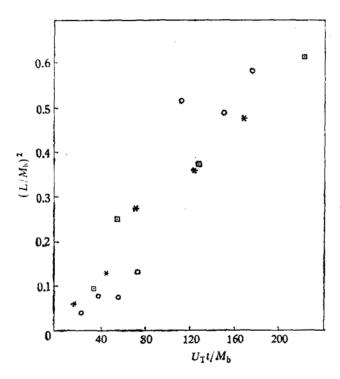


Fig. 8. The variation of non-dimensional integral scale in the course of non-dimensional time  $U_T t/M_b$  for  $N_c = 1$  with 3  $M_b(cm)$ : \*, 2.5;  $\circ$ , 4.0; m, 6.0.

are confirmed. The scatters existing in all the above figures may be attributed both to the uncertainties or errors in experiments and to the slight deviation of practical bubble turbulence from ideal homogeneous turbulence.

The asssistance of Zheng Cai-yun in preparing the experiments is gratefully acknowledged.

### REFERENCES

- [1] Levich, W. C., Physicochemical Hydrodynamics, Prentice-Hall Inc., Englewood Cliffs, N. J., 1962, 176-470.
- [2] Batchelor, G. K., The Theory of Homogeneous Turbulence, The University Press, Cambridge, England, 1956.
- [3] Turner, J. S., J. Fluid Mech., 33(1968), 290.
- [4] Britter, R. E. et al., ibid., 127(1983), 27.
- [5] Hopfinger, E. J., J. Geophys. Res., C5(1987), 92:5287.
- [6] Helsronl, G., Handbook of Multiphase Systems Hemisphere, Washington, 1962.
- [7] Liu, Y. N., Jia F. & Chen, X. W., Acta Mechanica Sinica, 3(1991), 257.
- [8] Dickey, T. D. & Mellor, G. L., J. Fluid Mech., 99(1980), 13.
- [9] Batchelor, G. K. & Townsend, A. A., Proc. Roy. Soc., 193A (1948), 539.